AIP | Applied Physics Letters

Ultrasonic fingerprint sensor using a piezoelectric micromachined ultrasonic transducer array integrated with complementary metal oxide semiconductor electronics

Y. Lu, H. Tang, S. Fung, Q. Wang, J. M. Tsai, M. Daneman, B. E. Boser, and D. A. Horsley

Citation: Applied Physics Letters **106**, 263503 (2015); doi: 10.1063/1.4922915
View online: http://dx.doi.org/10.1063/1.4922915
View Table of Contents: http://scitation.aip.org/content/aip/journal/apl/106/26?ver=pdfcov
Published by the AIP Publishing

Ultrasonic fingerprint sensor using a piezoelectric micromachined ultrasonic transducer array integrated with complementary metal oxide semiconductor electronics

Y. Lu,[1] H. Tang,[2] S. Fung,[1] Q. Wang,[1] J. M. Tsai,[3] M. Daneman,[3] B. E. Boser,[2] and D. A. Horsley[1]
[1]*Berkeley Sensor and Actuator Center, University of California, Davis, 1 Shields Avenue, Davis, California 95616, USA*
[2]*Berkeley Sensor and Actuator Center, University of California, Berkeley, California 94720, USA*
[3]*InvenSense, Inc., 1745 Technology Drive, San Jose, California 95110, USA*

(Received 13 April 2015; accepted 20 May 2015; published online 29 June 2015)

This paper presents an ultrasonic fingerprint sensor based on a 24×8 array of 22 MHz piezoelectric micromachined ultrasonic transducers (PMUTs) with 100 μm pitch, fully integrated with 180 nm complementary metal oxide semiconductor (CMOS) circuitry through eutectic wafer bonding. Each PMUT is directly bonded to a dedicated CMOS receive amplifier, minimizing electrical parasitics and eliminating the need for through-silicon vias. The array frequency response and vibration mode-shape were characterized using laser Doppler vibrometry and verified via finite element method simulation. The array's acoustic output was measured using a hydrophone to be ~14 kPa with a 28 V input, in reasonable agreement with predication from analytical calculation. Pulse-echo imaging of a 1D steel grating is demonstrated using electronic scanning of a 20×8 sub-array, resulting in 300 mV maximum received amplitude and 5:1 contrast ratio. Because the small size of this array limits the maximum image size, mechanical scanning was used to image a 2D polydimethylsiloxane fingerprint phantom (10 mm × 8 mm) at a 1.2 mm distance from the array. © *2015 AIP Publishing LLC*. [http://dx.doi.org/10.1063/1.4922915]

Over the past two decades, a variety of physical mechanisms have been exploited to capture an electronic image of a human fingerprint, including optical, capacitive, pressure, and acoustic mechanisms.[1] Among these, capacitive fingerprint sensors[2] are the ones most widely used in consumer electronics because they are fabricated using conventional complementary metal oxide semiconductor (CMOS) integrated circuit technology.[3] However, capacitive fingerprint sensors are extremely sensitive to contamination and moisture on the finger. Ultrasonic fingerprint sensors offer a potential solution to this problem, because the fingerprint's valleys and ridges are easily distinguished due to the great difference between their acoustic impedance (430 Rayl for an air-filled valley and ~1.5 MRayl for a ridge's human tissue). In addition, ultrasonic pulse-echo imaging has the potential to be more secure as it allows images to be collected at various depths beneath the epidermis, providing images of the sub-surface dermis layer and blood vessels. However, previous ultrasonic fingerprint sensors[4] were based on a single, mechanically scanned, focused ultrasonic transducer, resulting in large size, low frame-rate, and high cost. Micromachined ultrasonic transducers (MUTs), originally developed for medical ultrasound applications, solve these problems and a fingerprint sensor based on capacitive MUTs (CMUTs) has been reported.[5] Here, we demonstrate an ultrasonic fingerprint sensor based on piezoelectric MUTs (PMUTs) that are fully integrated with CMOS circuitry. Whereas a CMUT is based on capacitive electrodes separated by a submicron vacuum gap, a PMUT consists of a solid piezoelectric capacitor, greatly simplifying fabrication and improving mechanical robustness. While earlier PMUTs have been based on PZT[6] and ZnO,[7] the PMUTs demonstrated here are based on piezoelectric aluminum nitride (AlN), a material that is compatible with CMOS fabrication and used in low-cost, high-volume devices such as bulk-acoustic wave filters.[8] The sensor's electronic architecture and performance are described in Ref. 9; here, we focus on electromechanical and acoustic characterization and demonstrate ultrasound imaging of 1D and 2D phantoms.

Fig. 1 shows a cross-sectional system diagram. The device is fabricated by bonding a CMOS wafer (containing the circuitry) to a MEMS wafer (containing the PMUT array) using a conductive AlGe eutectic bond.[10] Fig. 2 shows a

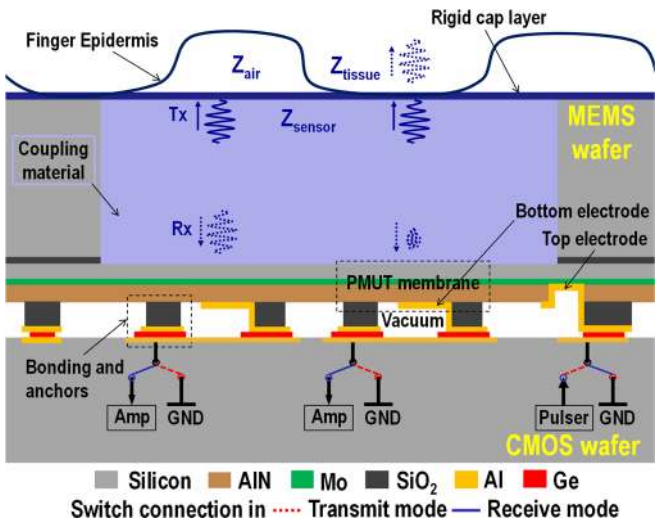

FIG. 1. Cross-sectional system diagram.

top-view optical image of the device after de-bonding the MEMS and CMOS dice along with a cross-sectional scanning electron microscope (SEM) image of a single PMUT. Each PMUT is a piezoelectric unimorph composed of a 6 μm thick Si elastic layer, 200 nm thick Mo top electrode layer, 800 nm thick AlN piezoelectric layer, and 200 nm thick Al bottom electrode layer. A 2.5 μm thick annular SiO_2 standoff is anchored to the CMOS wafer by the AlGe bonding layer, which defines the 50 μm diameter PMUT's mechanical boundary and provides electric contact between each PMUT and the CMOS circuitry beneath. A single AlGe bond at the bottom of each column of 8 PMUTs provides a contact to that column's top electrode layer, while individual annular AlGe bond rings provide a contact to the circular bottom electrode of each PMUT. While MUT-CMOS integration has been achieved using through-silicon vias and solder-ball flip-chip bonding,[6,11] here the bonding is conducted at wafer-scale and without the need for costly through-silicon vias, both dramatically reducing manufacturing costs and risks. The same manufacturing process has been used to realize PMUT arrays having cylindrical acoustic waveguides above the PMUT array.[12] After bonding, the MEMS wafer is thinned to 220 μm thickness by mechanical grinding and a plasma etch is used to expose the PMUT's Si elastic layer. After dicing, assembly, and wire-bonding, the etched region of each chip is subsequently filled with a coupling layer that has acoustic impedance similar to that of human tissue. In experiments presented here, a liquid coupling layer (Fluorinert FC-70) is used for convenience, however, gels and polymer layers such as PDMS (polydimethylsiloxane) are also suitable coupling layers;[13] the coupling layer can be capped by a hard lid composed of a material such as polyethylene or polystyrene with suitable acoustic impedance.

The fingerprint image is detected from differences in the acoustic reflection arising from impedance mismatch at the surface of the coupling layer, $R = (Z_2 - Z_1)/(Z_1 + Z_2)$, where Z_1 is the acoustic impedance of coupling medium and Z_2 is that of the material on the sensor's surface. Using a coupling layer with impedance $Z_1 = 1.3$ MRayl, the reflection from a fingerprint ridge with $Z_2 = 1.5$ MRayl (tissue) is

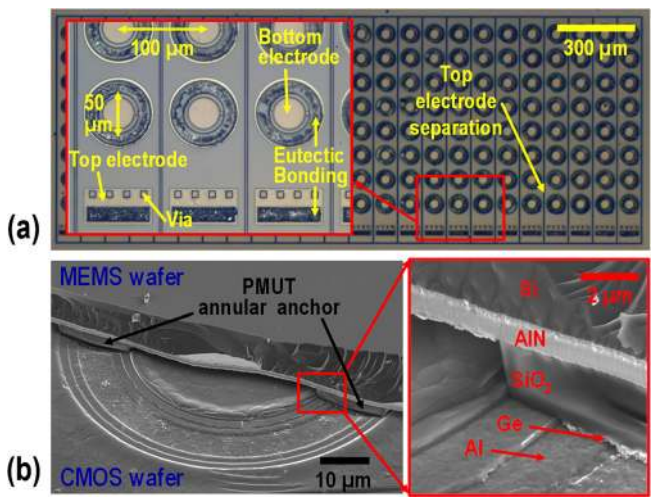

FIG. 2. (a) Optical images of the 24 × 8 PMUT array after de-bonding to remove the CMOS wafer; (b) cross-sectional SEM images of a single PMUT after partial de-bonding to remove the MEMS wafer.

$R = 7\%$, while $R \approx 100\%$ for a valley with $Z_2 = 430$ Rayls (air). A typical ridge width is 500 μm, which is ~3× of valley width, and therefore spreading loss from the ridge is ~3× smaller of that from the valley, resulting in a theoretical contrast ratio of ~5:1 = (100%):(7% × 3). Pulse-echo ultrasound images are collected by first transmitting an ultrasonic plane wave by exciting all the PMUTs in the 24 × 8 array with a 28 V 2-cycle 22 MHz square-wave. The pulse length and operating frequency were selected to achieve the desired axial and lateral resolution;[14] with a 2-cycle 22 MHz pulse, the theoretical axial resolution in tissue is 68 μm, while the lateral resolution is 60 μm, as discussed below. Transmit/receive switches on the CMOS die are used to connect the external pulser ASIC[13] to the common top electrode layer, while the individual bottom electrode of each PMUT is grounded through another set of switches (Fig. 1). Acoustic echoes are then received by connecting the bottom electrodes to individual receive amplifiers beneath each PMUT using the same switches. This connection scheme isolates the high-voltage transmit amplifier (which has large output capacitance) from the charge collection node connected to the receive amplifier. The PMUT's capacitance, $C_0 = 90$ fF, is small and therefore any stray capacitance on this node reduces the PMUT's receiving sensitivity. The stray capacitance, estimated to be $C_P = 44$ fF and dominated by the capacitance of the AlGe bonding region, is minimized by the close proximity of the receive amplifier to the PMUT.

Electromechanical testing was conducted first in air, using a scanning laser Doppler vibrometer (LDV, OFV-5000, Polytec, Inc.) to measure the mode-shape and displacement amplitude of a 5 × 5 subarray of PMUTs as a function of frequency. Frequency response measurements were collected using a 10 V chirp signal with a frequency range from 27.7 MHz to 29.5 MHz, corresponding to ~28 mV amplitude at a single frequency. Fig. 3 shows an image of the array's first resonance mode, occurring at 28.4 MHz in air with a quality factor $Q_{air} = 111$. The resonance frequency of the 25 PMUTs within this subarray varied by less than 0.2% (28.352 MHz–28.385 MHz), while the displacement amplitude at resonance varied by a larger amount of 26%. The histogram shows that 22 of the 25 PMUTs measured have displacement sensitivity in the range from 1.5 nm/V to 2 nm/V, with an average value of 1.8 nm/V. Some of the variation in amplitude may be due to the 7 μm step-size used in capturing the mode-shape; based on the measured mode-shape, a shift of 7 μm relative to the PMUT center would result in a 15% reduction in the measured displacement amplitude. A finite element method (FEM) model for the PMUT displacement predicted a static displacement of 33 pm/V, which when scaled by Q_{air} is approximately 50% greater than the average experimentally observed value. We observed that a lithography error resulted in top electrode metal outside of the desired electrode area; this error may be responsible for the reduced amplitude and large variation.

The PMUT array was wire bonded on a printed circuit board (PCB). Acoustic tests were then conducted with the array immersed in fluid with a 0.04 mm needle hydrophone (Precision Acoustics, Inc.) used to measure the pressure field generated by the array. The measured pressure amplitude is ~14 kPa peak-to-peak when the hydrophone was scanned

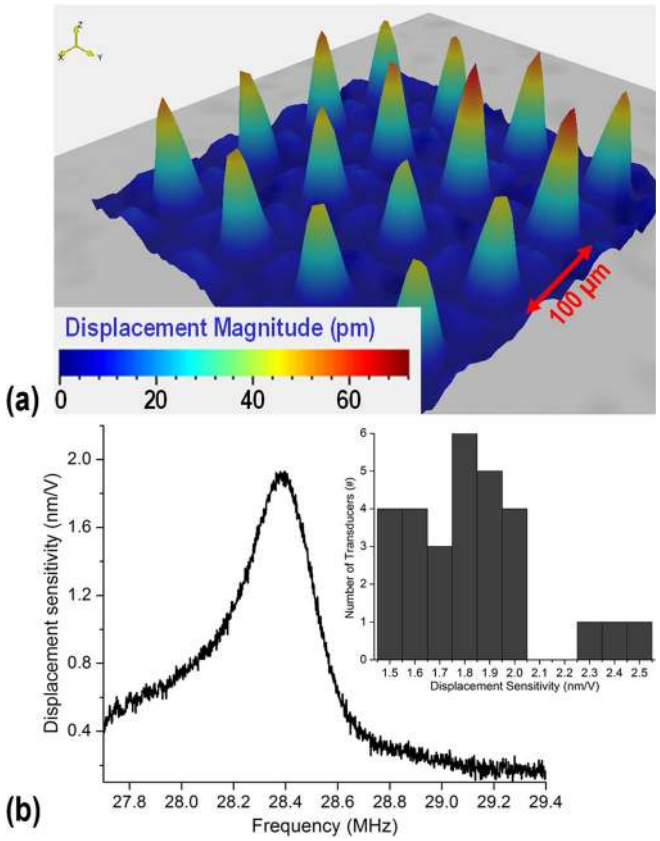

FIG. 3. (a) Mode-shape of a 5×5 sub-array measured at 28.4 MHz using a scanning LDV; (b) displacement frequency response of the 25 PMUTs. Inset: histogram of the peak displacement sensitivity for the 25 PMUTs tested.

over a distance of ~300 μm from the PMUT array. A FFT of the measured time-domain pressure signal showed an 11.5 MHz 3-dB bandwidth at a 22 MHz center frequency, corresponding to a quality factor $Q_f \approx 2$. Note that the resonance frequency (22 MHz) in fluid is lower than that (28.4 MHz) in air due to the increased mass of the fluid load.[15] The measured pressure amplitude can be compared with the LDV-measured displacement using a simple model for the ideal plane-wave pressure generated by a surface oscillating with amplitude d_f at frequency f, $P = (2\pi f d_f) Z_f A_e \sqrt{F}$, where the first term in parentheses represents the velocity of oscillation, $Z_f = 1.3$ MRayl is the acoustic impedance of the fluid, $F = 17\%$ is the array's fill-factor, and $A_e = 1/3$ is a factor that accounts for the fact that the PMUT's vibration mode-shape is not that of a pure piston.[16] Scaling the LDV-measured displacement (1.8 nm/V) by the input voltage (28 V) and the ratio of the quality factor in fluid to that in air (2/111), the expected displacement amplitude in fluid is 1 nm, and the pressure equation yields an estimate of 22 kPa peak-to-peak, in reasonable agreement with the measured pressure, given that the short 700 μm length of the array results in a non-ideal plane-wave.

Imaging tests were conducted first using a one-dimensional grating with 185 μm lines and 215 μm spaces etched into a steel foil placed on top of the PMUT array and immersed in fluid. A 20×8 sub-array is driven to transmit an ultrasonic plane wave, and a 20×1 row of PMUTs in the middle of the array is used to detect the returning echoes. Fig. 4 shows a 1D pulse-echo ultrasonic image of the grating measured using electronic scanning of the receiving PMUTs. The second echo can be observed arriving at ~2 μs, roughly twice the first echo's time of arrival. The maximum received voltage was ~300 mV_{pp}. Reducing the transmit voltage from 28 V to 7 V reduces the received signal level by approximately the same factor (4×) but has been shown to yield a 12 dB SNR for pulse echo imaging.[9] The received amplitude is in reasonable agreement with the theoretical voltage amplitude, estimated using $P = 14$ kPa (measured pressure) to be $v_{echo} = 249$ mV_{pp} using the following equation:

$$v_{echo} = A_v (C_0/C_{amp}) S (w/z)^{0.5} RP,$$

where A_v is the voltage gain of the second- and third-stage amplifiers (100), C_0 is the PMUT capacitance (90 fF), C_{amp} is the capacitance of the front-end charge amplifier (100 fF), S is the PMUT's receiving sensitivity (0.6 μV/Pa), w is the half-width of the grating line (92.5 μm), z is the propagation distance from the grating to the PMUT (340 μm), and $R = 63\%$ is the reflection ratio of steel with $Z_1 = 1.3$ MRayl (fluid) and $Z_2 = 5.8$ MRayl (steel). Using diffraction theory, a 185 μm line is expected to be increased by $z\lambda/(2w) \approx 60$ μm, where $\lambda = 34$ μm is the wavelength of sound at 22 MHz in Fluorinert FC-70, resulting in an image with 245 μm lines and 155 μm spaces. However, the resolution limit of the 100 μm pitch array makes the line and space widths appear approximately equal in the image.

The maximum fingerprint area that can be imaged via electronic scanning is equal to the size of the array (2.3 mm × 0.7 mm), as previously demonstrated.[9] To capture a larger image, mechanical scanning was performed to collect an image of a fingerprint phantom with ~600 μm pitch, similar to that of a human fingerprint. The phantom is a PDMS (Z = 1.5 MRayl) stamp with an artificial fingerprint pattern. Air-filled valleys in the pattern are sealed by a 250 μm thick PDMS sheet, as shown in Fig. 5(a). To perform pulse-echo imaging, a pulsed plane wave is launched from the 24×8 PMUT array and only a single PMUT at the center of the array is used to detect the reflected echoes. The phantom is located 1.2 mm from the PMUT array, immersed in fluid and then mechanically scanned above the PMUT array with a

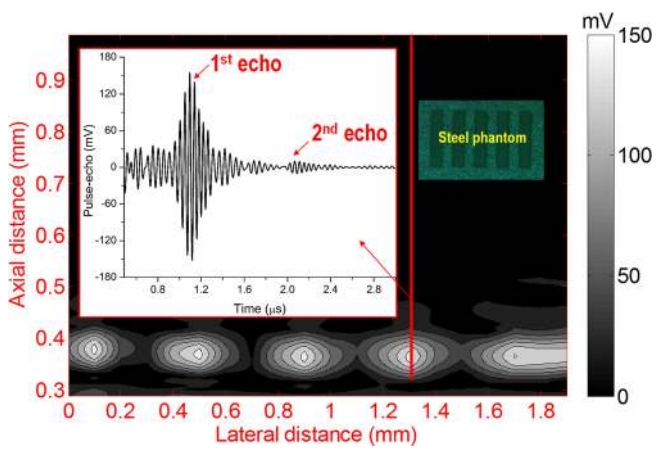

FIG. 4. 1D Pulse-echo ultrasonic imaging of a steel phantom using electronic scanning: inset pictures are the time-domain pulse-echo response and an optical image of the steel phantom.

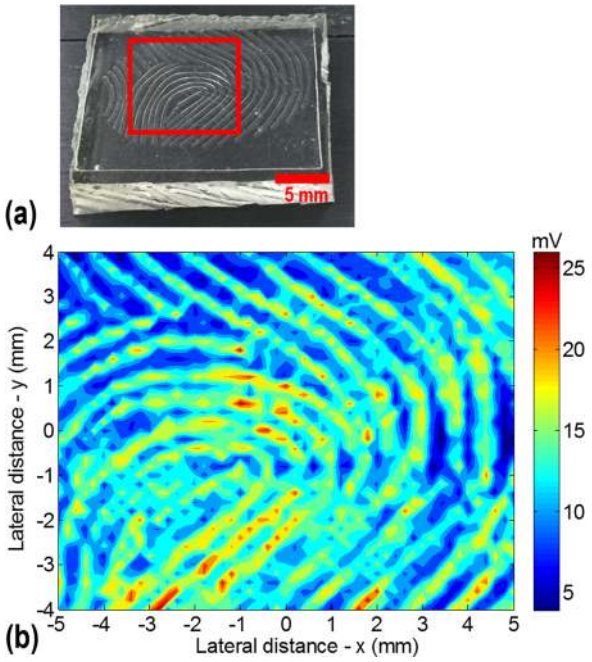

FIG. 5. (a) Fingerprint phantom made from patterned PDMS sealed with a PDMS sheet; (b) 2D pulse-echo ultrasonic image of the PDMS fingerprint phantom.

100 μm step-size. The captured image, Fig. 5(b), plots the amplitude of the received echo signal, which has maximum value of ~25 mV. The 35% variation in amplitude may be due to sample tilt and poor adhesion between the PDMS sheet and the patterned block in the center of the phantom. The contrast ratio is reduced to ~2.5 due to increased spreading from diffraction and scattering over the 1.2 mm path length.

In conclusion, we demonstrated an ultrasonic fingerprint sensor based on a 24×8 array of AlN PMUTs bonded to custom signal processing electronics fabricated in 180 nm CMOS technology. The 50 μm diameter, 22 MHz PMUTs have 0.1 mm pitch, resulting in an array size of 2.3 mm $\times$ 0.7 mm. Pulse-echo imaging is conducted by driving all the PMUTs in the array simultaneously with a 28 V 22 MHz 2-cycle pulse, producing a quasi-plane-wave with a pressure of 14 kPa. The returning echoes are received using on-chip receive amplifiers and digitized off-chip for subsequent analysis. An image of a 1D steel grating demonstrated the ability to image features with a minimum width of 200 μm, while a 2D PDMS fingerprint phantom was imaged at a distance of 1.2 mm from the array. The 0.1 mm pitch of this array was determined by the PMUT diameter required to achieve a center frequency of ~20 MHz. Reducing the thickness of the PMUT's 6 μm Si layer would allow smaller PMUT diameter and therefore finer pitch at the same operating frequency, while also resulting in lower Q and therefore higher bandwidth.

The authors thank Qing Zhou and Professor Alexander Revzin at UC Davis for PDMS phantom fabrication, InvenSense, Inc., for device fabrication, and Berkeley Sensor and Actuator Center (BSAC) Industrial Members for financial support.

[1]S. Memon, M. Sepasian, and W. Balachandran, in *International Multitopic Conference* (2008), p. 226.
[2]J. W. Lee, D. J. Min, J. Kim, and W. Kim, IEEE J. Solid-State Circuits **34**(4), 469 (1999).
[3]J. M. Nam, S. M. Jung, and M. K. Lee, Sens. Actuators A **135**(1), 283 (2007).
[4]J. K. Schneider and S. M. Gojevic, in *IEEE Ultrasonics Symposium (IUS)* (2001), p. 595.
[5]N. Lamberti, G. Caliano, A. Iula, and A. S. Savoia, Sens. Actuators A **172**(2), 561 (2011).
[6]D. E. Dausch, K. H. Gilchrist, J. B. Carlson, S. D. Hall, J. B. Castellucci, and O. T. von Ramm, IEEE Trans. Ultrason. Ferroelectr. Freq. Control **61**(10), 1754 (2014).
[7]Q. F. Zhou, C. Sharp, J. M. Cannata, K. K. Shung, G. H. Feng, and E. S. Kim, Appl. Phys. Lett. **90**(11), 113502 (2007).
[8]R. C. Ruby, P. Bradley, Y. Oshmyansky, A. Chien, and J. D. Larson, in *IEEE Ultrasonics Symposium* (2001), p. 813.
[9]H. Tang, Y. Lu, S. Fung, J. M. Tsai, M. Daneman, D. A. Horsley, and B. E. Boser, in International Conference on Solid-State Sensors, Actuators & Microsystems (Transducers), Alaska, 2015.
[10]J. M. Tsai, M. Daneman, B. Boser, D. Horsley, M. Rais-Zadeh, H. Y. Tang, Y. Lu, O. Rozen, F. Liu, M. Lim, and F. Assaderaghi, in International Conference on Solid-State Sensors, Actuators & Microsystems (Transducers) (2015).
[11]I. O. Wygant, X. Zhuang, D. T. Yeh, O. Oralkan, A. S. Ergun, M. Karaman, and B. T. Khuri-Yakub, IEEE Trans. Ultrason. Ferroelectr. Freq. Control **55**(2), 327 (2008).
[12]Y. Lu, H. Tang, Q. Wang, S. Fung, J. M. Tsai, M. Daneman, B. E. Boser, and D. A. Horsley, Appl. Phys. Lett. **106**(19), 193506 (2015).
[13]H. Tang, Y. Lu, S. Fung, D. A. Horsley, and B. E. Boser, in *International Solid State Circuits Conference*, San Francisco (2015), p. 210.
[14]N. M. Tole and H. Ostensen, *Basic Physics of Ultrasonographic Imaging* (World Health Organization, 2005).
[15]J. J. Bernstein, S. L. Finberg, K. Houston, L. C. Niles, H. D. Chen, L. E. Cross, K. K. Li, and K. Udayakumar, IEEE Trans. Ultrason. Ferroelectr. Freq. Control **44**(5), 960 (1997).
[16]D. Blackstock, *Fundamentals of Physical Acoustics* (John Wiley & Sons, 2000).